J. Basic. Appl. Sci. Res., 3(8)443-456, 2013

ISSN 2090-4304
Journal of Basic and Applied Scientific Research
www.textroad.com

Preparation, Characterization of $NiFe_2O_4$ Nanoparticles Supported on Clinoptilolite and Optimization of Photocatalytic Degradation of Pollutants in Textile Wastewater by Taguchi Experimental Design

Reza Marandi[1], Amir Abdollah Mehrdad Sharif[2], Mohammad Ebrahim Olya[3], Reza Moradi[4*]

[1]Department of Environmental Engineering, Faculty of Engineering, Islamic Azad University, North Tehran Branch, Tehran, Iran
[2]Department of Analytical Chemistry, Faculty of Chemistry, Islamic Azad University, North Tehran Branch, Tehran, Iran
[3]Department of Environmental Research, Institute for Color Science and Technology, Tehran, Iran
[4]Department of Applied Chemistry, Faculty of Chemistry, Islamic Azad University, North Tehran Branch, Tehran, Iran

ABSTRACT

In the present work, the precipitation method has been used to stabilize $NiFe_2O_4$ nanoparticles on Clinoptilolite (CP). $NiFe_2O_4$/CP catalysts have been characterized by scanning electron microscopy (SEM), X-ray diffraction (XRD), Fourier transform infrared spectroscopy (FT-IR) and BET surface area analysis. Optimum process conditions were determined for the removal of pollutants from textile wastewater using the Taguchi fractional design method. Four controllable factors containing pH, photocatalyst amount, H_2O_2 concentrations and volumetric flow rate were identified for the removal of pollutants at four levels for each factor. The optimum conditions were as follows: pH, 3; photocatalyst amount (mg/l), 75; H_2O_2 concentration (ppm), 55; and volumetric flow rate (l/min), 1.5. Main and interaction effects were analyzed by analysis of variance (ANOVA), F-test to define most important process variables affecting the removal of pollutants from textile wastewater. COD analysis of the pollutants under optimum conditions showed 82% reduction in COD in a 60 min period. The TOC analysis showed that all organic substances in the textile wastewater is converted into minerals.

KEYWORDS: Textile wastewater, Photocatalytic degradation, $NiFe_2O_4$/Clinoptilolite, Experimental design.

1. INTRODUCTION

Different types of dyes have been extensively used in industry for applications such as textiles, leathers, papers, foodstuffs, additives, gasoline, cosmetics, xerography, laser materials, and so on (Dakiky and Nemcova 2000; Bhaskar et al., 2003; Isak et al., 2000; Karpicz et al., 2000; Navarro and Sanz 1999; Tao et al., 1999).

Specified amounts of dye are lost in the process of manufacturing and utilization and often cause environmental pollution problems.

The wastewaters generated by the textile industry contain considerable amounts of azo dyes. The discharge of these coloured wastewaters in the ecosystem has been problematic due to their toxicity and resistance to biodegradability. Among Different techniques for the removal of coloured compounds, the traditional ones, such as adsorption, extraction, ultra-filtration, coagulation–flocculation, ozonation, H_2O_2 oxidation, photo-oxidation, and combination of several techniques have been applied (Gong et al., 2005; Madaeni and Mansourpanah 2004; Guibal and Roussy 2007; Nikazar et al., 2007). A lot of experiments have focused on the use of photocatalytic oxidation techniques for wastewater treatment. The mechanism involving photocatalytic oxidation processes has been extensively discussed in the literature (Turchi and Ollis 1988; Sabate et al., 1991; Nikazar et al., 2008; Matthews and McEvoy 1992).

There is a wide range of applications for the Taguchi method, from engineering and agriculture to chemistry (Donmez et al., 1998; Copur et al., 1997; Abali et al., 1997; Khoei et al., 2002; Tortum et al., 2005; Yesilyurt 2004; Hesampour et al., 2008). The use of the Taguchi method in ordinary experimental

[*]**Corresponding Author:** Reza Moradi, Department of Applied Chemistry, Faculty of Chemistry, Islamic Azad University, North Tehran Branch, Tehran, Iran. Tel.: +98 2122977932, Fax: +98 2122977861, E-mail address: r_moradi@iau-tnb.ac.ir

design methods, and keeping the experimental cost at a lowest level, will minimize the product diversity response but keeps the average response to objective. Another benefit is that optimal experimental conditions can be used in the real environment (Ross 1998). In this method organic compounds can be completely decomposed to H_2O and CO_2 by photocatalysis and no secondary pollutants are generated. The aim of the present study is to evaluate photocatalytic degradation of textile wastewater by using photocatalyst. The degradation of this textile wastewater has been previously studied by the use of UV/H_2O_2 (Arjomandirad et al., 2012). Zeolite seems to be a promising support for nickel ferrite ($NiFe_2O_4$) photocatalyst because of its regular pores and channel sizes, and good adsorption ability. $NiFe_2O_4$ supported on CP integrates the photocatalytic activity of $NiFe_2O_4$ with the adsorption properties of CP together, which induce a synergistic effect, resulting in the enhancement of photocatalytic efficiency. $NiFe_2O_4$ possess magnetic properties which increase photocatalytic activities.

The scientific contribution of this paper are: 1) the process offers great potential as an industrial technology to detoxify wastewaters; 2) Wastewater treatment sectors and textile industry will benefit from the results. In the present work $NiFe_2O_4$ has been stabilized on Clinoptilolite. The precipitation method has been used to perform the experiment. Therefore, determined optimum process conditions for the removal of pollutants from textile wastewater using the Taguchi fractional design method.

2. MATERIALS AND METHOD

2.1. Materials

The raw materials were Iranian Clinoptilolite (CP) (Afrand Tuska Company, Iran) extracted from deposits in the region of Semnan. Clinoptilolite chemical compounds by EDX standard quantification analysis are shown in Table 1.

Samples of textile industrial wastewater were obtained from Boroujerd textile factory (Iran-Boroujerd).

Other chemicals used in the project were purchased from the Merck Company (Germany).

2.2. Preparation of $NiFe_2O_4$ Immobilized on Clinoptilolite

Other researchers have already described the preparation method of $NiFe_2O_4$ nano- particles(Xu et al., 2007) With this method, for preparing of $NiFe_2O_4$ nanoparticles were initially prepared using 2.5M $Fe(NO_3)_3$ and 1.25M $Ni(NO_3)_2$ solutions. Then they were mixed with 60 ml of each solution and 6M NaOH solution was added slowly into the mixture solution until pH 10 was obtained. At this stage dropwise $FeCl_2$ solution (1M) was added into the mixture until the mole ratio of Fe^{2+}/Fe^{3+} 0.02 was obtained. By the dropwise addition of NaOH solution (6M), the pH value of the resulting mixture was adjusted to ca. 10.0. This mixture was refluxed for 2 h. For several times solid phases were washed with de-ionized water and were separated using the centrifuge method. In this method, $NiFe_2O_4$ nanoparticles, was mixed with CP using ethanol (1:2:1w/w %) as a solvent using agate pestle and mortar. This material was dried at 110 ^{0}C in an oven for 2 h and calcined in air at 700 ^{0}C for 4 h. The precipitation was sieved using 100 mesh standard sieve.

2.3. Apparatus

Figure 1 shows the schematic diagram of Circulating Fludized Bed Reactor (C.F.B.R) which was used for photocatalytic decomposition of textile wastewater. In this equipment, the total volume of photoreactor was 3 liters with three lamp (mercury 15W, low pressure, Philips) was used in photoreactor. UV/VIS Spectrophotometer, Jenway (6505) was employed for measuring absorbance using glass cells of path length 1 Cm. XRD analysis of the samples was done using a X-ray diffractometer Philips-XPert MPD, tube: Co kα , wavelength: λ=1.78897Å , Voltage: 40 kV, Current: 30 mA. The morphologies and specific surface areas of the photocatalyst were taken using a Philips XL30 scanning electron microscope (SEM) with EDX analyzer, FT-IR spectroscopy PerkinElmer, TOC analyzer Shimadzu 5000 and a Micrometric-100E Brunauer Emmett Teller (BET).

2.4. Procedures

For the photodegradation of pollutants, a sample wastewater solution containing pollutant and a specific amount of photocatalyst was used. The suspension pH values were adjusted at the desired level using dilute NaOH and H_2SO_4 (the pH values were measured with Horiba M12 pH meter) and then were allowed to equilibrate for 30 min in darkness. Then the prepared suspension was transferred to a 3.5 liter Pyrex tank. The photodegradation reaction took place under the radiation of Mercury lamp in 3

photoreactors as is shown in the, schematic diagram Figure 1. The concentration of the samples was determined using a spectrophotometer (UV-vis spectrophotometer, Jenway (6505). The degree of photodegradation (X) as a function of time is given by:

$$X = \frac{C_\circ - C}{C_\circ} \quad (1)$$

Where $C_\circ$ and C are the concentration of pollutants in wastewater at t = 0 and t, respectively.

COD analysis was done by the standard acid dichromate method (APHA and AWWA 1989).
For determination of optimal condition, the Taguchi experiment design was used. This method included the following steps:

1- The effective variables on the test results were determined.
2- Levels of each variable was identified separately (interaction between variables was to be considered).
3- The suitable orthogonal array (O.A.) and the assignment of process parameters to the orthogonal array were chosen.
4- On the basis of (O.A.), the required experiments were carried out.
5- The statistical analysis was done.
6- The ANOVA statistical procedure was used to analysis the results of the experiment.

The study was done to determine the optimal process conditions for removing the pollutants from textile wastewater. The effect of experimental parameters on the removal of pollutants and their levels are given in Table 2.
In this study the design of experiments and the analysis was done using Qualitek-4 software.
Orthogonal array the experimental design method was chosen to determine the experimental plan, as seen Table 3 (Ross 1998).
In order to see the effects of noise- sources- removing pollutants, each test was repeated three times under the same conditions. Optimizing statistical function was chosen as indicators. Three classes of statistical function were larger - better, smaller - better and naminal are the best. In this research, the statistical function, larger - better was used to define the optimal conditions (Ross 1998).
The larger - better statistical function was given by Eq. (2).

$$SN_L = -10\log\left(\frac{1}{n}\sum_{i=1}^{n}\frac{1}{Y_i^2}\right) \quad (2)$$

Where SN_L is statistical function, n the number of repetition done for an experimental combination, and Y_i the function value of i, th experiment.
In the Taguchi Experiment design method, the experiment corresponding to optimum experiment conditions might not have been done during the whole period of the experimental stage. In such cases, the function amount corresponding to optimum test conditions can be predicted by utilizing the balanced characteristic of O.A. . For this, the additive model may be used Eq. (3) (Ross 1998):

$$Y_i = \mu + X_i + e_i \quad (3)$$

where μ is the overall mean of performance value; X_i the fixed effect of the parameter level combination used in i, th experiment and e_i the random error in i, the experiment.

3. RESULTS AND DISCUSSION

3.1. The Characterization of Photocatalyst

Figure 2 shows the SEM images of (a) CP, (b) $NiFe_2O_4$ nanoparticles and (c) $NiFe_2O_4$/CP. It seems that the $NiFe_2O_4$ nanoparticles take place on the surface of Clinoptilolite. Regarding the specified scale in the Figure 2, the size of particles is nanometer. The BET surface areas of CP, $NiFe_2O_4$ and $NiFe_2O_4$/CP calculated by BET equation were 480, 134, 392 m^2g^{-1}, respectively.

To reveal the interaction between the $NiFe_2O_4$ and the CP, the crystal structures of the raw CP and the $NiFe_2O_4$/CP calcined at 700 ^{0}C after 4 h were measured as is shown in Figure 3. The XRD patterns of samples are illustrated in the Figure 3. XRD patterns of the as-prepared samples (2θ ranges from 10° to

80°). Clearly the XRD patterns of $NiFe_2O_4$/CP consist of the raw CP which can be calcined at 700 ^{0}C for 4 h. It is implied that the frame structure of zeolite after $NiFe_2O_4$ loading will not be destructed and less amount of $NiFe_2O_4$ has loaded on CP. The comparison of XRD patterns of $NiFe_2O_4$(Xu et al., 2007; Jiang et al., 2009; Sivakumar et al., 2011) before and after being calcined at 700 ^{0}C indicated that the crystalline phase of the prepared $NiFe_2O_4$ (supported on Clinoptilolite) and Clinoptilolite (Nikazar et al., 2008; Li et al., 2005; Huang et al., 2008) was stable during the heat treatment process. The crystallite size of $NiFe_2O_4$/CP was calculated using the Debye-Scherer formula:

$$D= 0.9 \lambda / \beta \cos\theta \quad (4)$$

where D is the average crystallite size, λ is the wavelength of Co kα , β is the full width at half maximum (FWHM) of the diffraction peaks, and θ is the Bragg's angle. The average crystallite size of $NiFe_2O_4$ supported on CP was estimated about 64 nm.

The EDX spectrum image, CP Zeolite, $NiFe_2O_4$ and $NiFe_2O_4$/Cp is presented in Figure 4. As it can be seen, elemental of each peak has been identified. EDX analysis of $NiFe_2O_4$ shows that the Weight and molar ratio of nickel to iron is 1:2 respectively.

Figure 5 shows the FT-IR spectra of CP, $NiFe_2O_4$ and $NiFe_2O_4$/Cp in the wave number range from 450 of 4000 cm^{-1}. The absorption bands around 1500 to 3500 cm^{-1} has been observed in all the spectra. The stretching vibrations of O-H group have emerged about 3400-3500 cm^{-1}. The strongest absorption peak at 1084.28 cm^{-1} is assigned to the framework stretching vibration band of Si(Al)-O in tetrahedral $Si(Al)O_4$ in natural zeolite, its position is unchanged at 700 ^{0}C treatment temperature, indicating that zeolite structure is not destroyed at 700 ^{0}C. The structural bands at 450-900 cm^{-1} are responsible for the stretching vibrations of T-O, T-O-T, and O-T-O bonds in tetrahedral SiO_4 and AlO_4. A new absorption band is found in the FT-IR spectra of $NiFe_2O_4$/Cp within the area of 1637.71 cm^{-1} which are corresponding to the stretching vibrations of Ni-O-Al and Ni-O-Si. Thus it can be concluded that the $NiFe_2O_4$ nanoparticles are well-established on CP. FT-IR spectra of CP is similar to the results from (Nikazar et al., 2008; Li et al., 2005; Huang et al., 2008) and FT-IR spectra of $NiFe_2O_4$ nanoparticles is similar to the results from(Sivakumar et al., 2011; Sivakumar et al., 2012; Mahmoodi 2013).

3.2. The Effect of Photocatalyst

Photocatalyst mechanism was used for the study since the ultraviolet radiation to the semiconducting oxides; electrons can be transferred from the valance to conduction bonds. During this transition, some holes are created in the valance bond and additional electrons are also created in the conduction bond. Dissolved oxygen molecules in water take extra electrons from the conduction bond and after some reaction, radical hydroxide will be released. On the other hand, after reaction with several holes the water molecules and the hydroxide ions are created in the valance bond, thus hydroxide radicals are created. Finally, hydroxide radicals with organic pollutants react and cause the breakdowns and failures, thus convert them into minerals.

The effect of different condition of degradation of pollutant in wastewater is shown in Figure 6. According to these results, pollutants can be degraded by hydrogen peroxide oxidation. This process can be accelerated with $NiFe_2O_4$/CP catalysts.

As indicated in Figure 6, because there are semiconductor oxides (TiO_2, Fe_2O_3 and MnO) in natural zeolite, there is a photocatalytic effect in this substance. Based on the experimental results, photocatalytic activity of $NiFe_2O_4$ after being stabilized on the CP zeolite increased.

As shown in Figure 7, the amount of photocatalytic reaction rate increases because it increases the speed of hydroxide radical's formation on ultraviolet irradiation.

3.3. The Effect of pH

pH is one of the main factors influencing the rate of degradation of some organic compounds in the photocatalytic process (Hofstandler et al., 1994; Anpo et al., 1986). It is also an important operational variable in actual wastewater treatment. As shown in Figure 8, photocatalytic decomposition of pollutants can be better done in acidic solution (Xu et al., 2007). Because of the reactions, hydroxide radical is formed and this facilitates it in the reaction.

$$e^-_{CB} + O_{2(ads)} \rightarrow {}^{\bullet}O^-_{2(ads)} \quad (5)$$

$${}^{\bullet}O^-_{2(ads)} + H^+ \rightarrow HO^{\bullet}_2 \quad (6)$$

$$2HO_2^{\bullet} \rightarrow O_2 + H_2O_2 \quad (7)$$

$$H_2O_2 + {}^{\bullet}O^-_{2(ads)} \rightarrow {}^{\cdot}OH + OH^- + O_2 \quad (8)$$

3.4. The Effect of H_2O_2 Concentration

As it can be seen in Figure 9, the decolorization rate increased when H_2O_2 concentration changed from 25 to 55 ppm. In H_2O_2 solution, the formation rate of hydroxyl radical was increased in two ways. First, symmetrical breaking of hydrogen peroxide molecule by illumination would also produce hydroxyl radicals. Second, the reduction of H_2O_2 in the conduction band would produce hydroxyl radicals (So et al., 2002; Lee et al., 2003).

$$H_2O_2 + h\upsilon \longrightarrow 2OH^{\bullet} \quad (9)$$

$$H_2O_2 + photocatalyst(e^-_{CB}) \longrightarrow photocatalyst + OH^{\bullet} + OH^- \quad (10)$$

3.5. The Effect of Volumetric Flow Rate

The results of the volumetric flow rate entering the reactor are shown in the diagram in Figure 10. As indicated in the diagram, first the volumetric flow rate increases to 1.5 l/min to remove the pollutants in the effluent, but then decreases.

The input volumetric flow rate reactors (the value 1.5 l/min), the number of contaminant molecules exposed to radiation and the amount of pollutants removed all seem to increase. With further increase in the volumetric flow rate (more than 1.5 l/min), turbulence in the flow increased too and the waste of radiation energy increased directionally with the increase of the amount of turbulence; where as the efficiency process reduced.

The optimum conditions were found to be as follows: pH,3; photocatalyst amount (mg/l), 75; H_2O_2 concentrations (ppm), 55; and volumetric flow rate (l/min), 1.5.

3.6. The Effect of Each Variable on Other Variables and Photocatalytic Decomposition of Pollutants

As it has been shown in Figure 11, based on the Taguchi experiment design the most effective parameter in the photocatalytic decomposition of pollutants is H_2O_2.

In Figure 12, the effect of each variable such as pH, H_2O_2 concentration, photocatalyst amount and volumetric flow rate on other variables has been defined. Based on the results of the experiment, the interaction between pH and photocatalyst amount has the highest value. It seems that the formation of $HO_2^{\bullet}$ is very dependent on the pH and catalyst. According to the reactions (6,7,8) hydroxide radicals were formed. Also in reactions (7,8) dissolved oxygen was formed that could react with electrons on conduction band to form hydroxide radicals.

3.7. Analysis of Variance (ANOVA) in Photocatalytic Degradation of Textile Wastewater

The influence and relative importance of these factors are quantitatively given by the analysis of variance (ANOVA). The results of ANOVA are listed in Table 4. The row which is marked as Other/error indicates the errors which are caused by uncontrollable factors (noise), that is factors which are not included in the experiment and experimental error. In general, the value should be below 50%, otherwise the results are not reliable. Here, the calculated error is about 4.436% which is far enough from the limit. The last column in Table 4, shows the percent contribution of each factor to the response. It is defined as the influence of one factor on the total observed variance in the experiment. A bigger value means that the factor contributes more to the final result. It can be seen that H_2O_2 has the biggest contribution between the factors. The optimum conditions are given by ANOVA. These conditions are determined according to the significances of the factors. This is expressed by the *F*-ratio which is defined as the ratio of variance due to the effect of a special factor on the variance compared to the error term. It means that the factors with an *F*-ratio less than one have no significant effect compared to the error. Table 5 shows the optimum conditions in textile wastewater according to variance ANOVA.

3.8. Photocatalytic Mineralization of Textile Wastewater

The chemical oxygen demand (COD) test is commonly used to indirectly measure the amount of organic compounds in textile wastewater. In this research, COD test was used to confirm that the organic pollutants are decomposed and are converted into mineral. The results of these experiments are shown in Figure 13.

The degradation of textile wastewater under optimal operational conditions and the removal 82% from organic pollutants have been performed in 60 min period. These results can be confirmed by the decomposition of organic matter that was present in the textile wastewater sample. The COD removal efficiency (%) has been calculated by:

$$\text{COD removal efficiency (\%)} = \frac{COD_{0} - COD}{COD_{0}} \times 100 \qquad (11)$$

Where COD_0 and COD are COD values at t = 0 and t, respectively.

3.9. The analysis of TOC in textile wastewater

Figure 14 shown TOC removal to analyze the textile wastewater. As it is clear, TOC amount has decreased with time increase which shows that analyzed organic substances in textile wastewater under optimal operational conditions and ultraviolet radiation have converted into minerals

Table 1: Clinoptilolite chemical compounds.

Formula	Conc.%
Na_2O	2.01
MgO	0.72
Al_2O_3	11.81
SiO_2	66.5
MnO	0.04
P_2O_5	0.01
K_2O	3.12
CaO	3.11
TiO_2	0.21
Fe_2O_3	1.3
Loss of ignition (L.O.I)	12.05

Table 2: Experimental parameters and their levels.

Factors	Level 1	Level 2	Level 3	Level 4
A) pH	3	5	7	9
B) Catalyst amount(mg/l)	25	50	75	100
C) H_2O_2 concentration(ppm)	25	35	45	55
D) Volumetric flow rate(l/min)	0.5	1	1.5	2

Table 3: Experimental plan table.

Experiments No	A	B	C	D
1	1	1	1	1
2	1	2	2	2
3	1	3	3	3
4	1	4	4	4
5	2	1	2	3
6	2	2	1	4
7	2	3	4	1
8	2	4	3	2
9	3	1	3	4
10	3	2	4	3
11	3	3	1	2
12	3	4	2	1
13	4	1	4	2
14	4	2	3	1
15	4	3	2	4
16	4	4	1	3

Table 4: Analysis of variance (ANOVA).

Factors	DOF [a]	Sum of Squares	Variance	F-Ratio	Pure Sum	Percent (%)		
pH	3	0.015	0.005	19.175	0.015	23.356	Cat	3
0.015	0.005	18.861	0.014	22.953				
H_2O_2	3	0.023	0.007	27.93	0.022	34.607		
v	3	0.01	0.003	12.399	0.009	14.648		
Other/error	4	0.009	0			4.436		
Total	16	0.072				100.0		

DOF [a]: Degree of freedom.

Table 5: Optimal conditions according to ANOVA

	Factors	Level Description	Level	Contribution
1	pH	3	1	0.014
2	Cat	75(mg/l)	3	0.011
3	H_2O_2	55(ppm)	4	0.033
4	v	1.5(l/min)	3	0.012

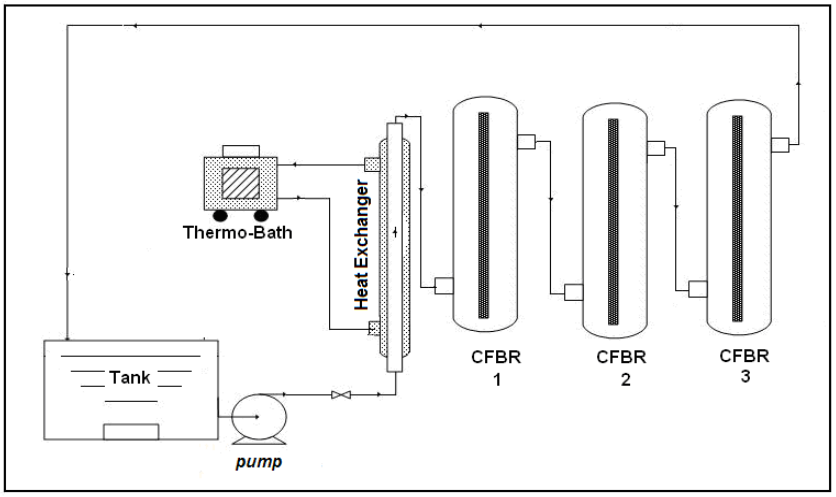

Figure 1. Schematic diagram of C.F.B.R.

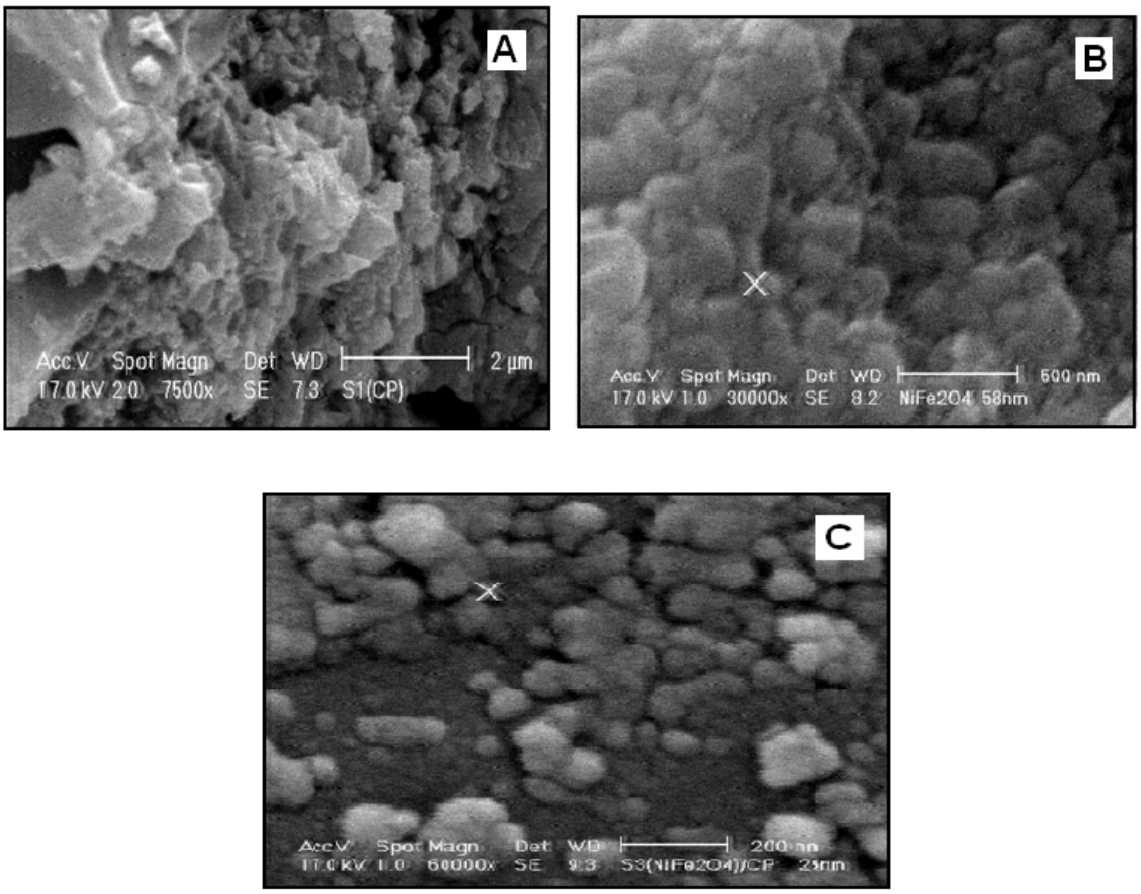

Figure 2. SEM images of (A) CP, (B) $NiFe_2O_4$ nano particles and (C) $NiFe_2O_4$/CP.

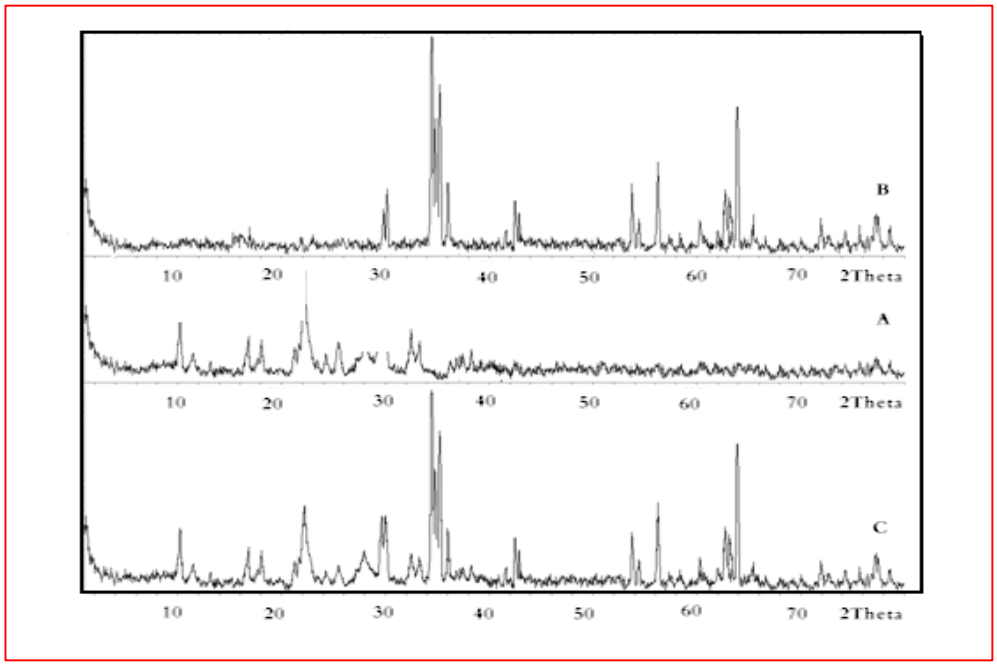

Figure 3. XRD pattern of (A) CP, (B) $NiFe_2O_4$ nano particles and (C) $NiFe_2O_4$/CP.

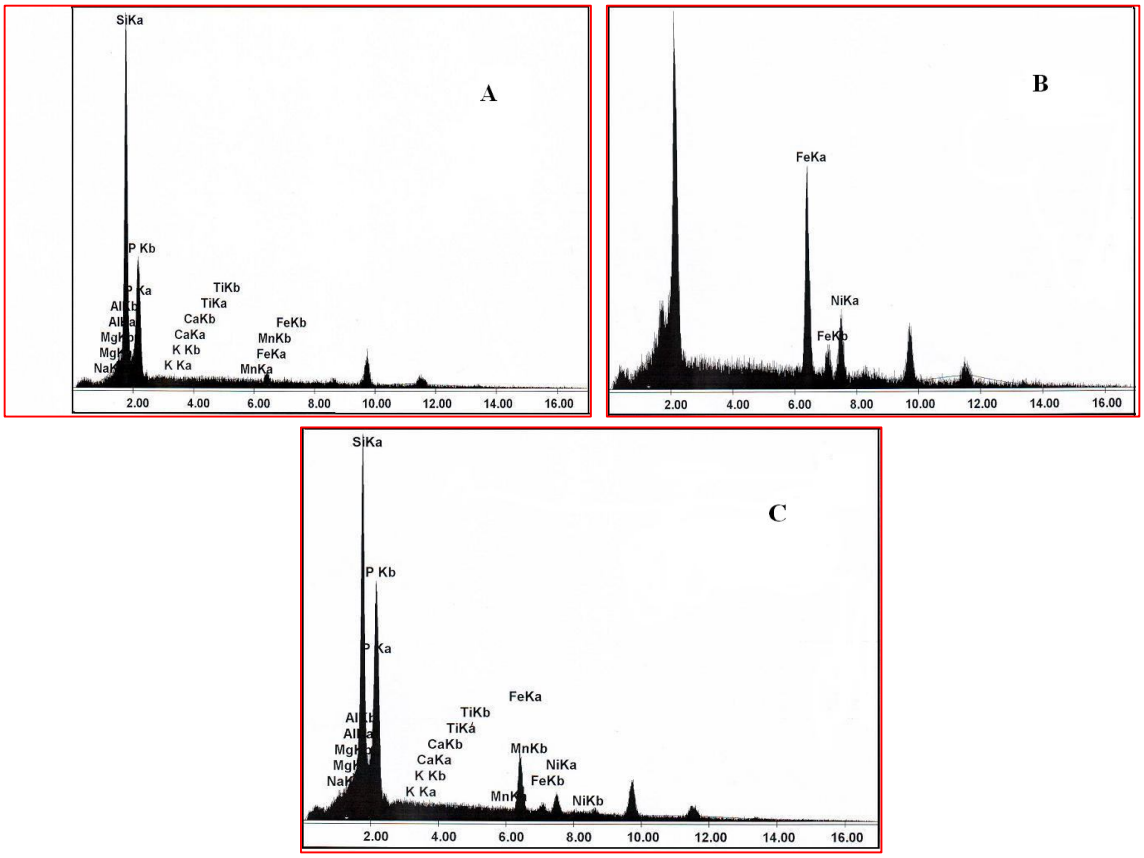

Figure 4. EDX spectrum image, (A) CP, (B) $NiFe_2O_4$ nano particles and (C) $NiFe_2O_4$/CP.

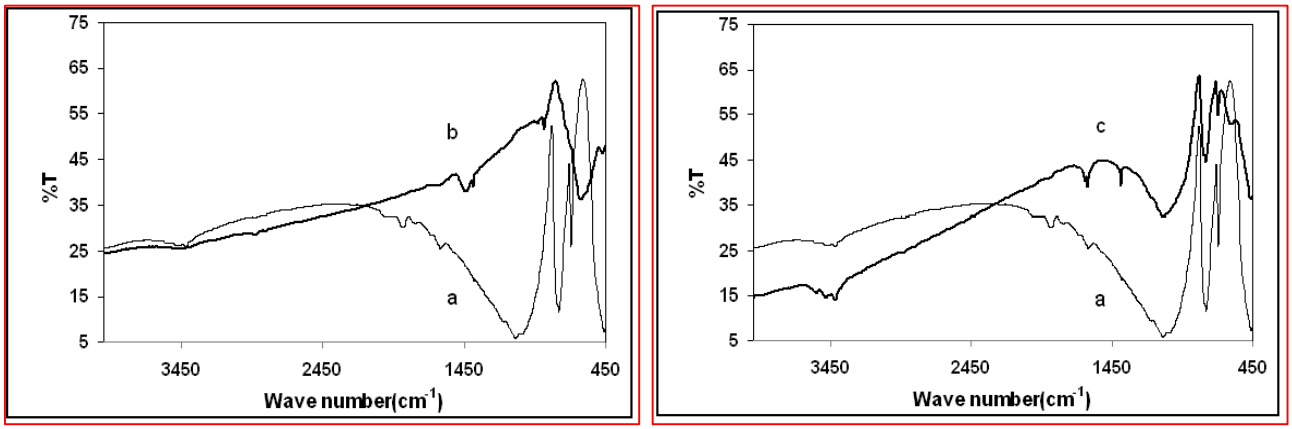

Figure 5. FT-IR spectra of (a) CP, (b) $NiFe_2O_4$ and (c) $NiFe_2O_4$/Cp

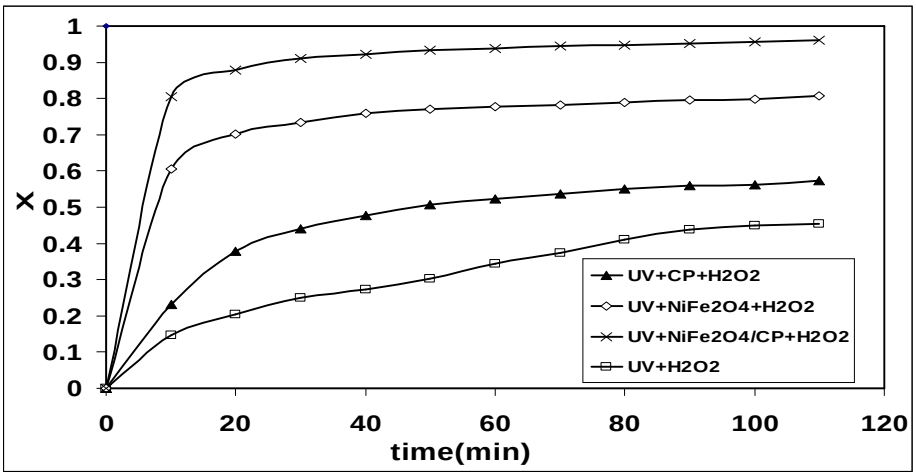

Figure 6. Effect of different conditions in degradation of pollutant in textile wastewater. pH= 3, photocatalyst amount =75(mg/l), H_2O_2 concentrations=55(ppm), volumetric flow rate =1.5(l/min), T=298(K).

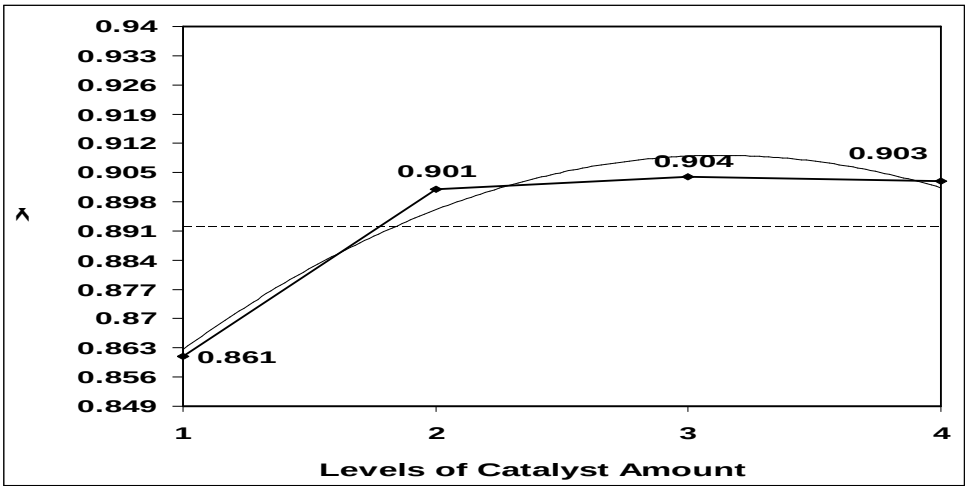

Figure 7. Effect of photocatalyst level in photodegradation of pollutants.

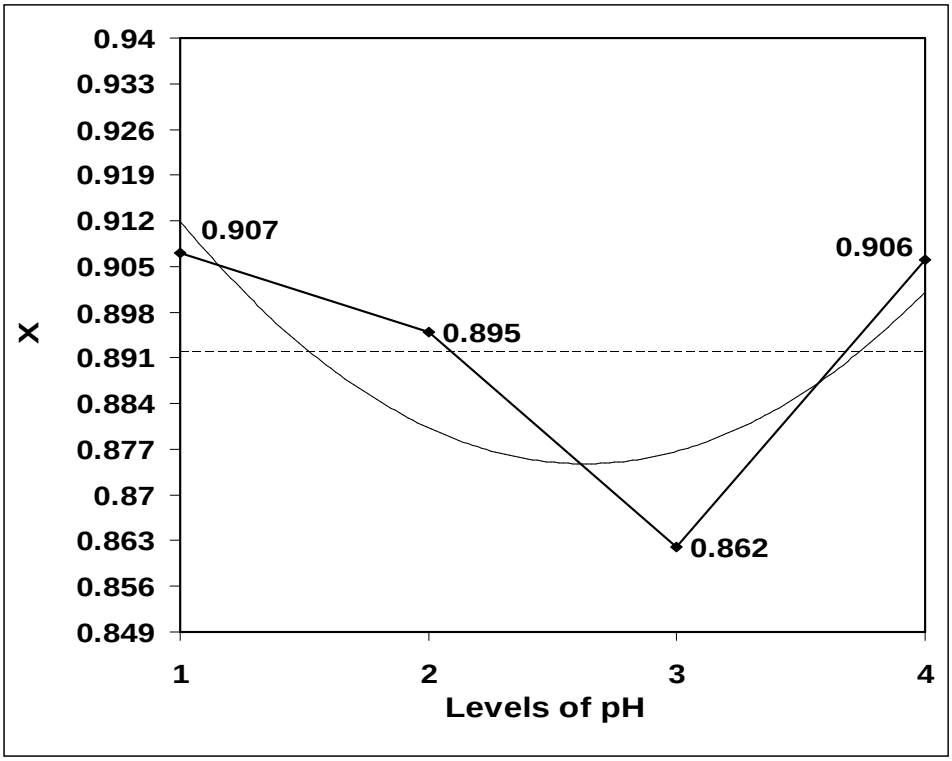

Figure 8. Effect of pH level in photodegradation of pollutants.

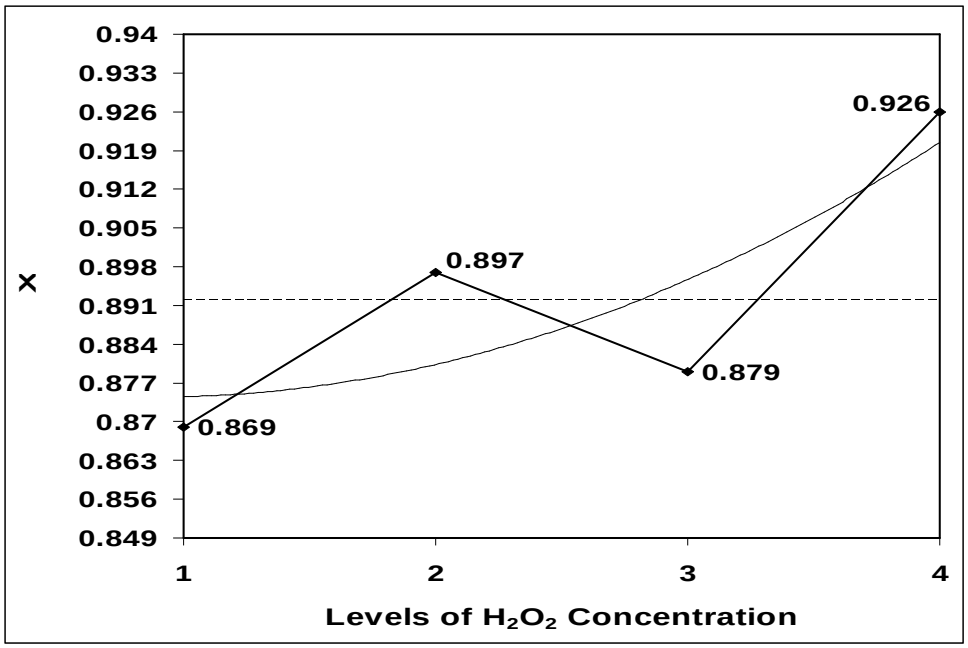

Figure 9. Effect of H_2O_2 concentration level in photodegradation of pollutants.

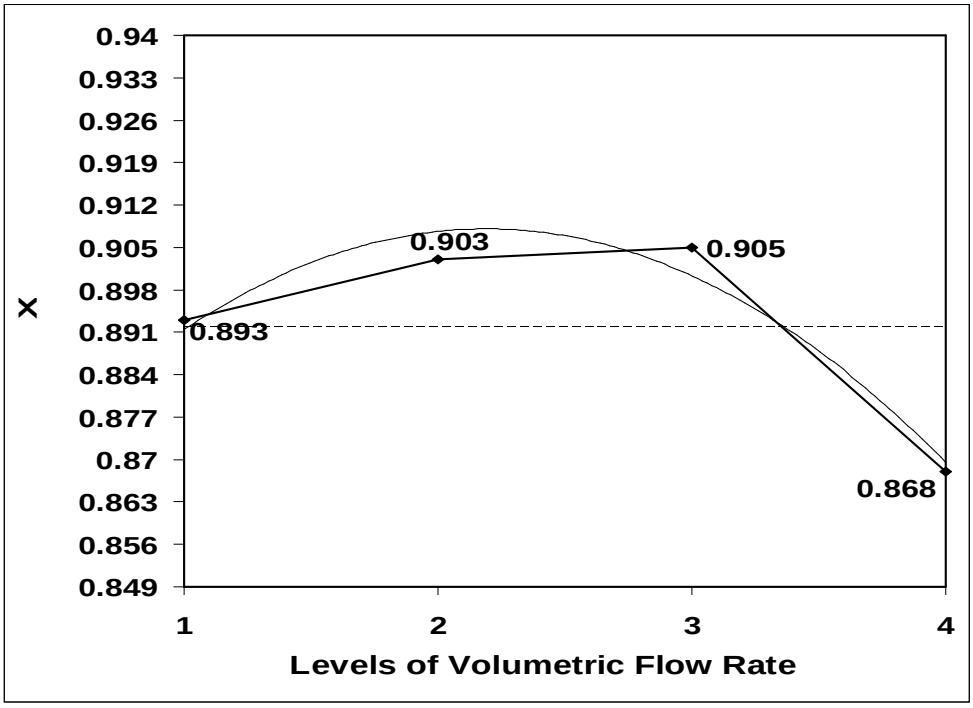

Figure 10. Effect of volumetric flow rate level in photodegradation of pollutants.

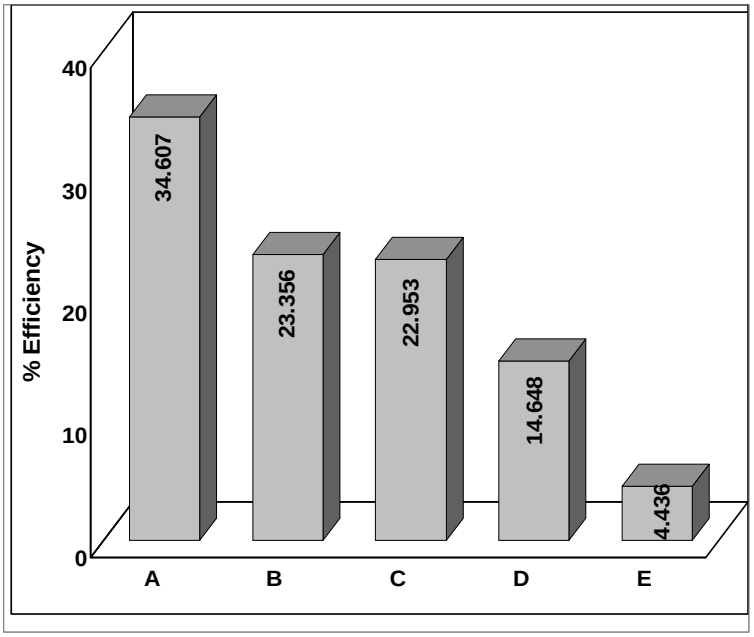

Figure 11. Effect of parameters on photocatalytic decomposition of pollutants.
A) H_2O_2 concentration, B) pH, C) Photocatalyst amount, D) Volumetric flow rate, E) Error.

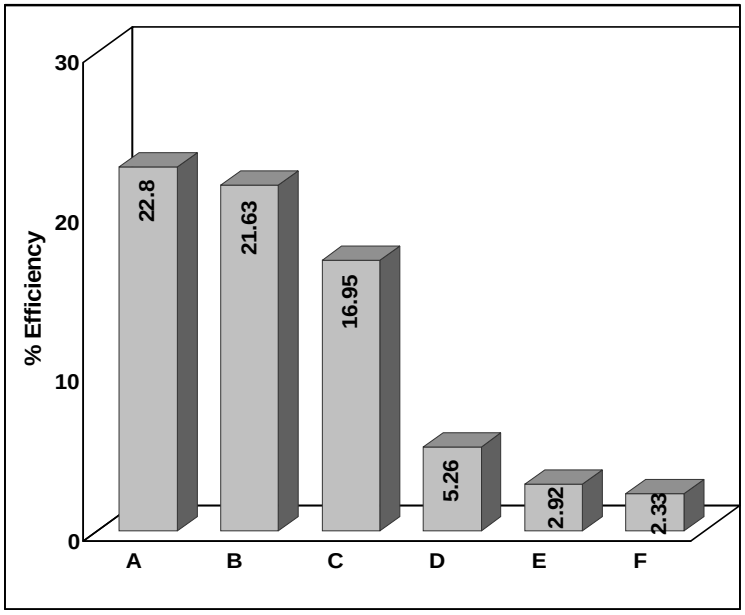

Figure 12. Effect of each parameter on other variables.
A)Effect of pH on photocatalyst amount, B) Effect of photocatalyst amount on volumetric flow rate, C) Effect of pH on volumetric flow rate, D) Effect of pH on H_2O_2 concentration, E) Effect of photocatalyst amount on H_2O_2 concentration, F) Effect of H_2O_2 concentration on volumetric flow rate.

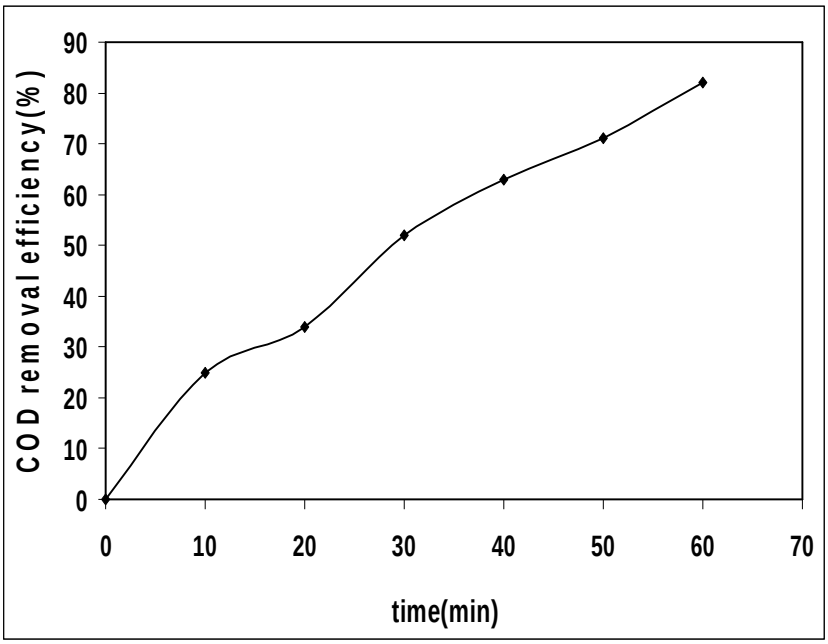

Figure 13. COD removal efficiency of textile wastewater.
pH= 3, photocatalyst amount =75(mg/l), H_2O_2 concentrations=55(ppm), volumetric flow rate =1.5(l/min), T=298(K).

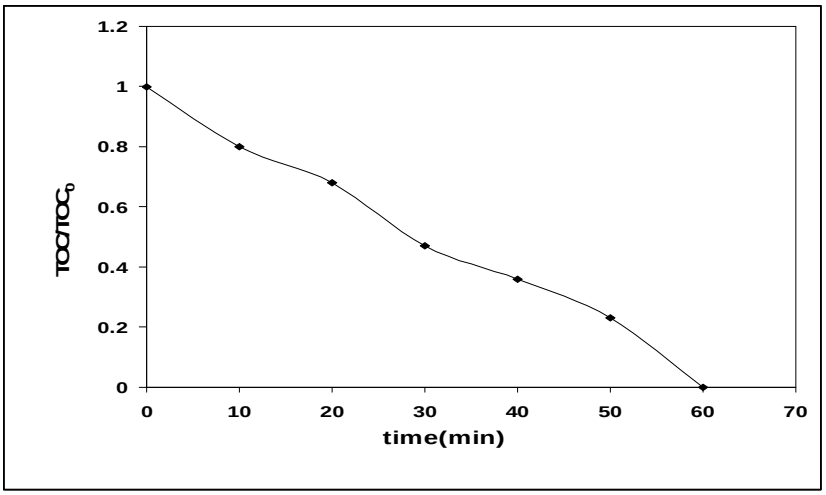

Figure 14. TOC removal of textile wastewater. pH= 3, photocatalyst amount =75(mg/l), H_2O_2 concentrations=55(ppm), volumetric flow rate =1.5(l/min), T=298(K).

4. CONCLUSIONS

Physical and chemical characterization of supported photocatalyst was determined by SEM, XRD, FT-IR, and BET techniques. According to the literature, the results demonstrated that the produced $NiFe_2O_4$/CP have sufficient properties as a photocatalyst for degradation of textile wastewater. Here, the Taguchi design method was used to optimize the parameter values for obtaining the desired characteristics. Various factors affecting the degradation process were analyzed and optimized. It has been shown that photocatalyst amount and pH highly affect the photocatalytic degradation of textile wastewater. Under the optimal conditions (pH=3, photocatalyst amount =75(mg/l), H_2O_2 concentrations=55(ppm), volumetric flow rate =1.5(l/min) as analyzed by the Taguchi method. The COD and TOC analysis showed that all organic pollutants in the textile wastewater is converted into minerals.

ACKNOWLEDGEMENTS

The authors wish to acknowledge members of the Research Laboratory of Islamic Azad University**,** Toyserkan Branch, Toyserkan, Iran and Boroujerd textile factory.

REFERENCES

Abali, Y., Colak, S., Yapici, S. 1997. The optimisation of the dissolution of phosphate rock with Cl_2 SO_2 gas mixtures in aqueous medium. *Hydrometallurgy* 46: 27-35.

APHA, AWWA, 1989. Standard methods for examination of water and wastewater. New York.

Arjomandirad, F., Ziaefar, N., Mehrabad, J.T. 2012. Removal of chromium(VI) from aqueous solutions by means of UV/TiO_2/H_2O_2 processes. *J. Basic Appl. Sci. Res.* 2(3):3016-3020.

Bhaskar, M., Gnanamani, A., Ganeshjeevan, R.J., Chandrasekar, R., Sadulla, S., Radhakrishnan, G. 2003. Analyses of carcinogenic aromatic amines released from harmful azo colorants by Streptomyces SP. SS07. *J. Chromatography A* 1018: 117-123.

Copur, M., Pekdemir, T., Celik, C., Colak, S. 1997. Determination of the Optimum Conditions for the Dissolution of Stibnite in HCl Solutions. *Ind. Eng. Chem. Res.* 36: 682-687.

Dakiky, M., Nemcova, I. 2000. Aggregation of o,o′- Dihydroxy azo Dyes III. Effect of cationic, anionic and non-ionic surfactants on the electronic spectra of 2-hydroxy-5- nitrophenylazo-4-[3-methyl-1-(4″-sulfophenyl)-5-pyrazolone]. *Dyes Pigments* 44: 181- 193.

Donmez, B., Celik, C., Colak, S., Yartasi¸ A. 1998. Dissolution Optimization of Copper from Anode Slime in H_2SO_4 Solutions. *Ind. Eng. Chem. Res.* 37: 3382-3387.

Gong, R., Li, M., Yang, C., Sun, Y., Chen, J. 2005. Removal of cationic dyes from aqueous solution by adsorption on peanut hull. *J. Hazard. Mater*. 121: 247-250.

Guibal, E., Roussy, J. 2007. Coagulation and flocculation of dye-containing solutions using a biopolymer (Chitosan). *React. Funct. Polym.* 67: 33-42.

Hesampour, M., Krzyzaniak, A., Nystrom, M. 2008. Treatment of wastewater from metal working by ultrafiltration, considering the effects of operating conditions. *Desalination* 222: 212-221.

Huang, M., Xu, C., Wu, Z., Huang, Y., Lin, J., Wu, J. 2008. Photocatalytic discolorization of methyl orange solution by Pt modified TiO_2 loaded on natural Zeolite. *Dyes Pigments* 77: 327-334.

Hofstandler, K., Kikkawa, K., Bauer, R., Novalic, C., Heisier, G. 1994. New Reactor Design for Photocatalytic Wastewater Treatment with TiO_2 Immobilized on Fused- Silica Glass Fibers: Photomineralization of 4-Chlorophenol. *Environ. Sci.Technol.* 28:670-674.

Isak, S.J., Eyring, E.M., Spikes, J.D., Meekins, P.A. 2000. Direct blue dye solutions: photo properties. *J. Photochem. Photobiol. A Chem.* 134: 77-85.

Jiang, J., Hong Ai, L., Chao Li, L., Liu, H. 2009. Facile fabrication and characterization of $NiFe_2O_4$/ZnO hybrid nanoparticles. *J. Alloys and Compounds* 484: 69–72.

Karpicz, R., Gulbinas, V., Undzenas, A. 2000. Picosecond Spectroscopic Studies of Tautomers of a Bisazo Compound in Solutions. *J. Chinese Chem. Soc.* 47: 589-595.

Khoei, A.R., Masters, I., Gethin, D.T. 2002. Design optimisation of aluminium recycling processes using Taguchi technique. *J. Mater. Process. Technol.* 127: 96 -106.

Lee, J.M., Kim, M.S., Hwang, B., Bae, W., Kim, B.W. 2003. Photodegradation of acid red 114 dissolved using a photo-Fenton process with TiO_2. *Dyes Pigments* 56: 59-67.

Li, F., Jiang, Y., Yu, L., Yang, Z., Hou, T., Sun, S. 2005. Surface effect of natural zeolite (clinoptilolite) on the photocatalytic activity of TiO_2. *Appl. Surf. Sci*. 252: 1410-1416.

Madaeni, S.S., Mansourpanah, Y. 2004. Chemical cleaning of reverse osmosis membranes fouled by whey. *Desalination* 161: 13-24.

Mahmoodi, N.M. 2013. Magnetic ferrite nanoparticle – alginate composite: Synthesis, characterization and binary system dye removal. *Journal of the Taiwan Institute of Chemical Engineers* 44: 322- 330.

Matthews, R.W., McEvoy, S.R. 1992. Photocatalytic degradation of phenol in the presence of near-UV illuminated titanium dioxide. *J. Photochem. Photobiol. A Chem.* 64: 231-246.

Navarro, A., Sanz, F. 1999. Dye aggregation in solution: study of C.I. direct red I. *Dyes Pigments* 40: 131-139.

Nikazar, M., Gholivand, K., Mahanpoor, K. 2007. Using TiO_2 supported on Clinoptilolite as a catalyst for photocatalytic degradation of azo dye Disperse yellow 23 in water. *Kinet. Catal.* 48: 230-236.

Nikazar, M., Gholivand, K., Mahanpoor, K. 2008. Photocatalytic degradation of azo dye Acid Red 114 in water with TiO_2 supported on clinoptilolite as a catalyst. *Desalination*219: 293-300.

Ross, P.J. 1998. Taghuchi techniques for quality engineering, McGraw-Hill, New York.

Sabate, J., Anderson, M.A., Kikkawa, H., Edwards, M., Hill Jr, C.G. 1991. A kinetic study of the photocatalytic degradation of 3- chlorosalicylic acid over TiO_2 membrane supported on glass. *J. Catal.* 127: 167-177.

Sivakumar, P., Ramesh, R., Ramanand, A., Ponnusamy, S., Muthamizhchelvan, C. 2011. Preparation of sheet like polycrystalline $NiFe_2O_4$ nanostructure with PVA matrices and their properties. *Materials Letters* 65: 1438–1440.

Sivakumar, P., Ramesh, R., Ramanand, A., Ponnusamy, S., Muthamizhchelvan, C. 2012. Synthesis, studies and growth mechanism of ferromagnetic $NiFe_2O_4$ nanosheet. *Appl. Surf. Sci.* 258: 6648-6652.

So, C.M., Cheng, M.Y., Yu, J.C., Wong, P.K. 2002. Degradation of azo dye Procion Red MX-5B by photocatalytic oxidation. *Chemosphere* 46: 905-912.

Tao, J., Mao, G., Daehne, L. 1999. Asymmetrical Molecular Aggregation in Spherulitic Dye Films. *J. Am. Chem. Soc.* 121: 3475-3485.

Tortum, A., Celik, C., Aydin, A.C. 2005. Determination of the optimum conditions for tire rubber in asphalt concrete. *Build. Environ.* 40: 1492-1504.

Turchi, C.S., Ollis, D.F. 1988. Photocatalytic reactor design: an example of mass-transfer limitations with an immobilized catalyst. *J. Phys. Chem.* 92: 6852-6853.

Xu, S., Shangguan, W., Yuan, J., Chen, M., Shi, J. 2007. Preparations and photocatalytic properties of magnetically separable nitrogen-doped TiO_2 supported on nickel ferrite. *Appl. Catal. B Environ.* 71: 177-184.

Yesilyurt, M. 2004. Determination of the optimum conditions for the boric acid extraction from colemanite ore in HNO_3 solutions. *Chem. Eng. Process.* 43: 1189-1194.